Collective excitations in HgTe-CdTe superlattices

1989 J. Phys.: Condens. Matter 1 7609

(http://iopscience.iop.org/0953-8984/1/41/012)

J. Phys.: Condens. Matter 1 (1989) 7609–7617. Printed in the UK

Collective excitations in HgTe–CdTe superlattices

Danhong Huang†, Yun Zhu‡ and Shixun Zhou†
† Department of Physics, Fudan University, Shanghai, People's Republic of China
‡ Centre of Theoretical Physics, China Centre of Advanced Science and Technology (World Laboratory), Beijing, and Department of Physics, Fudan University, Shanghai, People's Republic of China

Received 30 September 1988, in final form 17 January 1989

Abstract. We study the electron collective excitations of the HgTe–CdTe superlattice with a simple model, taking into account the overlap of wavefunctions at the interfaces for interface states. The linear-response theory has been used to calculate the dielectric response of the superlattice to an external perturbation, including many-body effects, magnetic fields and electron–phonon coupling in a reasonable way for both intra- and inter-sub-band modes.

1. Introduction

Recently, much attention has been paid to HgTe–CdTe superlattices which consists of both a semi-metal and a wide-gap semiconductor. The Γ_6–Γ_8 energy bands in HgTe are reversed, as shown in figure 1, in contrast with those in the CdTe layer, to give the zero gap. The computations of the band structure of the HgTe–CdTe superlattice given by the plane wave method (PWM) [1], the linear combination of atomic orbitals (LCAO) method [2, 3] and the envelope-function approximation (EFA) [4, 5] agree well and show that the electron-like, heavy-hole-like and light-hole-like states are, as expected, confined very well in the HgTe and CdTe layers [3, 6, 7]. On the contrary, the Γ_8 energy bands in the HgTe and CdTe layers possess effective masses with opposite signs on each side of the interface, respectively, which directly leads to the formation of a quasi-interface state with its energy E_i lying in the range $0 < E_i < \Lambda$, where $\Lambda = V_p$ is the separation of Γ_8 energy bands in the HgTe and CdTe layers. Clearly, the electrons in the HgTe layers will form quasi-interface states localised near the interface with energy $E_i < \Lambda$. Moreover, light holes in the CdTe layers will also form anomalous quasi-interface states localised near the interface, owing to the negative effective mass of the light hole. As a model of collective excitation, we can treat interface states in the HgTe and CdTe layers as two different kinds of quasi-particle with effective masses m_e and m_{lh}, respectively, just as the model given in [2, 4]. All these results are the consequences of matching the bulk states belonging to the conduction band in HgTe and the light-hole valence band in CdTe. This match is only favourable when the bulk states to be connected are made up of atomic orbitals of the same symmetry type and the effective masses on the two sides of the interface have the opposite sign.

It is proved that the thickness of the materials HgTe and CdTe will mainly determine the widths of band gap and sub-bands, respectively. We assume that the layers of HgTe

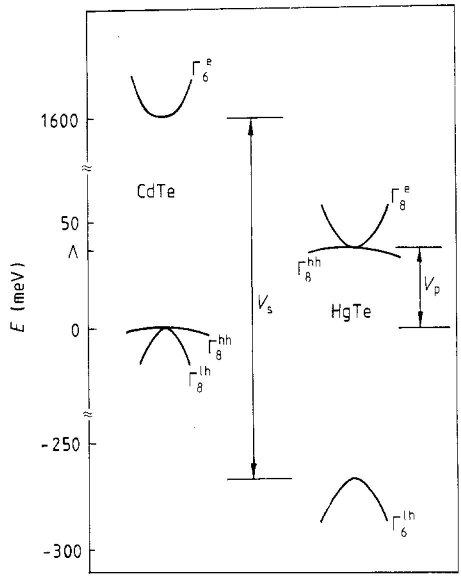

Figure 1. Band structure of bulk HgTe and CdTe. The superscripts lh, hh and e refer to light holes, heavy holes and electrons, respectively.

and CdTe have the same thickness $d/2$ and that d is smaller than the critical thickness d_c so that superlattice will behave like a semiconductor. We think that the interface states play a more important role in the HgTe–CdTe superlattice than in type I and type II superlattices. Also, we consider the motion of electrons in the layer to be completely free and, if d is not too small, we neglect tunnelling effects coming from the overlap of interface states localised at adjacent interfaces in the quantum well. Indeed, when the planar wavevector $\boldsymbol{k}_{\parallel}$ is not very small, the hybridisation between the interface states and the heavy-hole-like states will affect the fundamental gap of the material, which contributes a great deal to the transport and to optical absorption [4]. We have partly taken this effect into consideration by using wavefunctions with a finite width of localisation at interfaces. Generally, the effective mass $m_{\rm int}$ of the interface state will depend on the planar wavevector $\boldsymbol{k}_{\parallel}$. If the single-particle transitions are limited to the neighbourhood of the Γ point of energy bands in $\boldsymbol{k}$-space, the dominant term no longer depends on $\boldsymbol{k}_{\parallel}$ (the zeroth-order approximation), and then we can neglect the non-parabolic effect in the band structure [4]. In this case, the parabolic dispersion relation is still applicable.

The effect of hybridisation is reflected in three features: the finite width of localisation of interface states, the Coulomb interaction between the interface states and the heavy-hole-like states, and the non-parabolic energy dispersion relation. It should be pointed out that it is very difficult to calculate the analytical expression for the energy dispersion for both interface states and heavy-hole-like states with hybridisation. Fortunately, the effect of the non-parabolic energy dispersion relation cannot qualitatively change the collective excitation spectrum of interface states, although it contributes much to the transport and to optical absorption. Only the branch edges in the spectrum are quantitatively changed or shifted. The coupling between the interface and heavy-hole-like states also does not have much effect on the collective excitation spectrum of interface states. Only the optical plasmon mode intensity of heavy-hole-like state is reduced [8].

In § 2, we study the collective excitation spectrum of such a superlattice using the simple model which mainly concentrates on the effects of interface states.

2. The model system

We shall now discuss the linear response of a superlattice to an external potential for zero magnetic field. We write straightforwardly a series of basic self-consistent equations under the self-sustaining condition $V^{\mathrm{ext}} = 0$ and the electric quantum limit without repeating computations similar to those in [9, 10]:

$$
\begin{aligned}
\langle ns|V_0|0s'\rangle = {} & \sum_m \Pi_{m0}^{(3,3)}[(A + S_-B + S_+C)\langle m3|V_0|03\rangle + (S'_-B + S'_+C)\langle m3|V_1|03\rangle] \\
& + \sum_{i=1}^{3}\sum_m X_{m0}^{(i,i)}[V_{mn}^{H}(s's, ii) + S_-V_{mn}'^{H}(s's, ii) \\
& + S_+V_{nm}'^{H}(ii, ss')]\langle mi|V_0|0i\rangle + \sum_{i=3}^{4}\sum_m X_{m0}^{(i,i)} \\
& [S'_-V_{mn}'^{H}(s's, ii) + S'_+V_{nm}'^{H}(ii, s's)]\langle mi|V_1|0i\rangle \\
& + \sum_{\substack{i,j=1\\(i>j)}}^{3}\sum_m X_{m0}^{(i,j)}[V_{mm}^{H}(s's, ji) + S_-V_{mn}'^{H}(s's, ji) \\
& + S_+V_{nm}'^{H}(ji, s's)]\langle mi|V_0|0j\rangle + \sum_m X_{m0}^{(4,3)}[S'_-V_{mn}'^{H}(s's, 34) \\
& + S'_+V_{nm}'^{H}(34, s's)]\langle m4|V_1|03\rangle + \mathrm{LE}
\end{aligned} \tag{1}
$$

and

$$
\begin{aligned}
\langle ns|V_1|\,0s'\rangle = {} & \sum_m \Pi_{m0}^{(3,3)}[(A + S_-B + S_+C)\langle m3|V_1|03\rangle + (S'_-B + S'_+C)\langle m3|V_0|03\rangle] \\
& + \sum_{i=3}^{4}\sum_m X_{m0}^{(i,i)}[V_{mn}^{H}(s's, ii) + S_-V_{mn}'^{H}(s's, ii) + S_+V_{nm}'^{H}(ii, ss')] \\
& \times \langle mi|V_1|0i\rangle + \sum_{i=1}^{3}\sum_m X_{m0}^{(i,i)}[S'_-V_{mn}'^{H}(s's, ii) \\
& + S'_+V_{nm}'^{H}(ii, s's)]\langle mi|V_0|0i\rangle + \sum_{\substack{i,j=1\\(i>j)}}^{3}\sum_m X_{m0}^{(i,j)} \\
& \times [S'_-V_{mn}'^{H}(s's, ji) + S'_+V_{nm}'^{H}(ji, s's)]\langle mi|V_0|0j\rangle \\
& + \sum_m X_{m0}^{(4,3)}[V_{mn}^{H}(s's, 34) + S_-V_{mn}'^{H}(s's, 34) \\
& + S_+V_{nm}'^{H}(34, s's)]\langle m4|V_1|03\rangle + \mathrm{LE}
\end{aligned} \tag{2}
$$

with the symbols given by

$$V_{m0n}^{H(\pm)}(s's, p'p) = \frac{2\pi e^2}{\varepsilon_s q} \int \mathrm{d}z \int \mathrm{d}z' \exp(-q|z - z'|)$$
$$\times \psi_n^{(s)}(z)\psi_0^{(s')}(z)\psi_0^{(p')}(z' \mp d/2)\psi_m^{(p)}(z')\delta(p'p, 33) \qquad (3)$$

$$V'^{H(\pm)}_{m0n}(s's, p'p) = \frac{2\pi e^2}{\varepsilon_s q} \int \mathrm{d}z \int \mathrm{d}z' \exp[-q(z - z')]$$
$$\times \psi_n^{(s)}(z)\psi_0^{(s')}(z)\psi_0^{(p')}(z' \mp d/2)\psi_m^{(p)}(z')\delta(p'p, 33) \qquad (4)$$

$$V_{m0n}^{H}(s's, p'p) = \frac{2\pi e^2}{\varepsilon_s q} \int \mathrm{d}z \int \mathrm{d}z' \exp(-q|z - z'|)$$
$$\times \psi_n^{(s)}(z)\psi_0^{(s')}(z)\psi_0^{(p')}(z')\psi_m^{(p)}(z') \qquad (5)$$

$$V'^{H}_{m0n}(s's, p'p) = \frac{2\pi e^2}{\varepsilon_s q} \int \mathrm{d}z \int \mathrm{d}z' \exp[-q(z - z')]$$
$$\times \psi_n^{(s)}(z)\psi_0^{(s')}(z)\psi_0^{(p')}(z')\psi_m^{(p)}(z') \qquad (6)$$

and

$$A = V_{m0n}^{H(-)}(s's, 33) + V_{m0n}^{H(+)}(s's, 33) \qquad (7)$$

$$B = V'^{H(-)}_{m0n}(s's, 33) + V'^{H(+)}_{m0n}(s's, 33) \qquad (8)$$

$$C = V'^{H(-)}_{nm0}(33, s's) + V'^{H(+)}_{nm0}(33, s's) \qquad (9)$$

where LE stands for all the terms in either equation (1) or equation (2) which are obtained under the exchange of the indices m and 0 of the terms already presented. The labels $s = 1, 2, 3, 4$ refer to the electron-like, heavy-hole-like, interface and light-hole-like states, respectively. Here, in comparison with type I and type II superlattices, the additional terms $V_{m0n}^{H(\pm)}$ and $V_{nm0}^{H(\pm)}$ come from the overlap of wavefunctions at the interfaces for interface states. The non-interacting single-particle energy is given by (with $m_j^{(s)}$ as the mass for planar motion)

$$E_{n,j}^{(s)}(\boldsymbol{k}) = E_{n,j}^{(s)} + \hbar^2 k^2/2m_j^{(s)} \qquad (10)$$

where n is the sub-band index, and the layers are labelled by an integer j. Even-numbered layers will be taken to be the HgTe layers, while odd-numbered layers are the CdTe layers. Moreover, we have introduced in equations (1) and (2) the symbols $S_\pm$ and $S'_\pm$ defined by

$$S_\pm\ [\exp(-qd)\exp(\pm \mathrm{i}k_z d)]/[1 - \exp(-qd)\exp(\pm \mathrm{i}k_z d)] \qquad (11)$$

$$S'_\pm = [\exp(-qd/2)\exp(\pm \mathrm{i}k_z d/2)]/[1 - \exp(-qd)\exp(\pm \mathrm{i}k_z d)]. \qquad (12)$$

The irreducible polarisation under the random-phase approximation can be expressed as

$$\Pi_{nn',jj'}^{(s,s')}(\boldsymbol{q}, \omega) = \sum_{\boldsymbol{k}} \frac{f_0[E_{n'j'}^{(s')}(\boldsymbol{k}+\boldsymbol{q})] - f_0[E_{nj}^{(s)}(\boldsymbol{k})]}{E_{n'j'}^{(s')}(\boldsymbol{k}+\boldsymbol{q}) - E_{nj}^{(s)}(\boldsymbol{k}) - \hbar\omega}. \qquad (13)$$

We let the exchange–correlation potential V^{xc} be zero throughout this paper for convenience (i.e. the excitonic effects are neglected).

To obtain the intra-sub-band modes, we set $m = n = 0$ in equations (1) and (2). We shall first restrict our study to interface states (i.e. $s = s' = 3$). We choose for the symmetrical ground state

$$\psi_0^{(3)}(z) = \begin{cases} D\exp(kd/4)[\exp(kz) + \exp(-kd)\exp(-kz)] & -3d/4 \leqslant z \leqslant -d/4 \\ D\exp(-kd/4)[\exp(kz) + \exp(-kz)] & -d/4 \leqslant z \leqslant d/4 \\ D\exp(kd/4)[\exp(-kz) + \exp(-kd)\exp(kz)] & d/4 \leqslant z \leqslant 3d/4 \end{cases} \qquad (14)$$

with the normalisation factor

$$D = \exp(kd/4)/[d + 2\sinh(kd/2)/k]^{1/2} \qquad (15a)$$

and the long-wavelength form of $\chi_0^{e,h}(\boldsymbol{q}, \omega) = \boldsymbol{\Pi}_{00}^{e,h}(\boldsymbol{q}, \omega)$ given by

$$\chi_0^{e(h)}(\boldsymbol{q}, \omega) = n_{e(h)}q^2/m_{e(h)}\omega^2. \qquad (15b)$$

Here we set $k_{HgTe} = k_{CdTe} = k$ in the calculation for simplicity. The substitution of equation (14) into equations (1) and (2) reduces them to the form

$$\omega_\pm^2 = [\omega_{pe}(q)^2 + \omega_{ph}(q)^2][A + (S-1)B]/2 \pm \{[\omega_{pe}(q)^2 - \omega_{ph}(q)^2]^2 \times [A + (S-1)B]^2 + 4\omega_{pe}(q)^2\omega_{ph}(q)^2 S'^2 B^2\}^{1/2}/2 \qquad (16)$$

with

$$A = \{4[2 + \exp(-kd/2)]/[d + 2\sinh(kd/2)/k]^2\}\{2q/(q^2 - 4k^2) \times [\sinh(kd/2)/k + \sinh(kd)/4k + d/4] + [d + 2\sinh(kd/2)/k]/q - \{\exp[-(2k+q)d/4]/(2k+q) - \exp[(2k-q)d/4]/(2k-q) + 2\exp(-qd/4)/q\}\{\sinh[(2k+q)d/4]/(2k+q) + \sinh[(2k-q)d/4]/(2k-q) + 2\sinh(qd/4)/q]\} \qquad (17)$$

$$B = \{4[2 + \exp(-kd/2)]/[d + 2\sinh(kd/2)/k]^2\}\{\sinh[(2k+q)d/4]/(2k+q) + \sinh[(2k-q)d/4]/(2k-q) + 2\sinh(qd/4)/q\}^2 \qquad (18)$$

and the structure factors S and S' defined by

$$S(\boldsymbol{q}, k_z) = \sinh(qd)/[\cosh(qd) - \cos(k_z d)] \qquad (19)$$

$$S'(\boldsymbol{q}, k_z) = 2\cos(k_z d/2)\sinh(qd/2)/[\cosh(qd) - \cos(k_z d)]. \qquad (20)$$

In the weak-coupling limit ($qd \gg 1$), we obtain *localised bulk-like optical plasmons* (i.e. ω tends to a common constant for $q_z d = 0, \pi$ when $qd \gg 1$). This is very different from what happens in type I and type II superlattices, in which $\omega \sim q^{1/2}$ as $qd \gg 1$. In the strong-coupling limit ($qd \ll 1$), we obtain *3D optical plasmon and acoustical modes*, for $k_z = 0$. When $k_z d = (2n+1)\pi$, we obtain *modulated 3D acoustical plasmons*, as shown

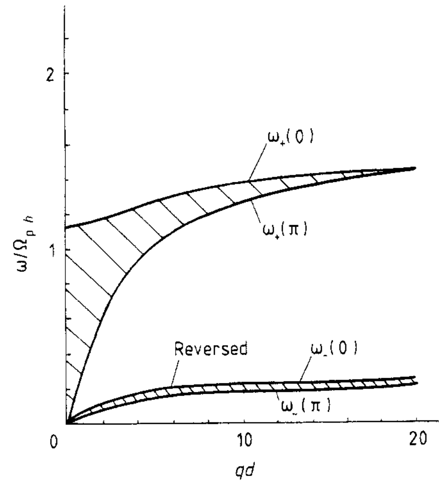

Figure 2. The collective intra-sub-band excitation spectrum of interface states in quasi-2D interfaces with the parameters $kd = 7.742$, $\omega_{pe}^2/\omega_{ph}^2 = 55.0$ and $\varepsilon_S = 10.0$.

in figure 2. The criterion for the transition behaviour from 2D ($\omega \sim q^{1/2}$) to 3D ($\omega \simeq$ constant) system as $qd \gg 1$ can be clearly described as follows: the screening length of Coulomb interaction should be much smaller than the width of localisation at the interfaces (i.e. $q^{-1} \ll k^{-1}$) to ensure sufficient overlap of the wavefunctions.

For the inter-sub-band modes, the anti-symmetrical excited interface states with a finite width of localisation take the form

$$\psi_1^{(3)}(z) = \begin{cases} C\exp(-kd/4)\{\exp[-k(z+d/2)] - \exp[k(z+d/2)]\} & -3d/4 \leqslant z \leqslant -d/4 \\ C\exp(-kd/4)[\exp(kz) - \exp(-kz)] & -d/4 \leqslant z \leqslant d/4 \\ C\exp(-kd/4)\{\exp[-k(z-d/2)] - \exp[k(z-d/2)]\} & d/4 \leqslant z \leqslant 3d/4 \end{cases} \tag{21}$$

where the normalisation factor is given by

$$C = \exp(kd/4)\,[2\sinh(kd/2)/k - d]^{1/2}$$

and the long-wavelength form of $\chi_1^{e(h)}(\boldsymbol{q},\omega) = \Pi_{10}^{e(h)}(\boldsymbol{q},\omega) + \Pi_{01}^{e(h)}(\boldsymbol{q},\omega)$ to the order of q is given by

$$\chi_1^{e(h)}(\boldsymbol{q},\omega) = 2n_{e(h)}\Omega_{10}/\hbar(\omega^2 - \Omega_{10}^2).$$

Substituting equation (21) into equations (1) and (2), we find that

$$\omega_\pm^2 = \Omega_{10}^{(3)2}\{1 + (\alpha_e + \alpha_h)[P + (S-1)Q]/qd\} \pm \{(\alpha_e - \alpha_h)^2[P + (S-1)Q]^2 + 4\alpha_e\alpha_h S'^2 Q^2\}^{1/2}\Omega_{10}^{(3)2}/qd \tag{22}$$

with

$$P = \{8/[4\sinh^2(kd/2)/k^2 - d^2]\}[2q[\sinh(kd) - kd]/4k(q^2 - 4k^2) + \{\exp[-(2k+q)d/4]/(2k+q) + \exp[(2k-q)d/4]/(2k-q)] \times [\sinh[(2k+q)d/4]/(2k+q) - \sinh[(2k-q)d/4]/(2k-q)]\} \tag{23}$$

$$Q = -\{8/[4\sinh^2(kd/2)/k^2 - d^2]\}[\sinh[(2k+q)d/4]/(2k+q) - \sinh[(2k-q)d/4]/(2k-q)]^2 \tag{24}$$

where

$$\alpha_{\mathrm{e(h)}} = [(2n_{\mathrm{e(h)}}/\hbar\Omega^{(3)}_{10})(2\pi e^2/\varepsilon_{\mathrm{s}})](d/2). \tag{25}$$

In the weak-coupling limit ($qd \gg 1$), as expected, each layer supports a common *localised 3D inter-sub-band mode* to exhibit the bulk-like properties. In the strong-coupling limit ($qd \ll 1$), we obtain two branches of coupled inter-sub-band modes for interface states, when $k_z = 0$. For $k_z d = (2n+1)\pi$, we find the modes in which the coupling has been totally screened out.

We now consider a static external magnetic field B_0 oriented along the z direction parallel to the superlattice axis. The effects of electron–phonon coupling can be taken into account by replacing the background dielectric constant ε_{s} with a frequency-dependent dielectric function

$$\varepsilon_{\mathrm{s}}(\omega) = \varepsilon_\infty(\omega^2 - \omega_{\mathrm{L}}^2)/(\omega^2 - \omega_{\mathrm{T}}^2) \tag{26}$$

where ω_{L} and ω_{T} are the longitudinal and transverse optical phonon frequencies. In this case, equations (1) and (2) can be solved for ω^2 to give

$$\omega^2 = \{\omega_{\mathrm{L}}^2 + \omega_{\mathrm{c}}^2 + [\omega_{\mathrm{p}}^{(3)}(q)]^2\gamma_\pm\}/2 \pm [\![\{\omega_{\mathrm{L}}^2 + \omega_{\mathrm{c}}^2 + [\omega_{\mathrm{p}}^{(3)}(q)]^2\gamma_\pm\}^2 - 4\{\omega_{\mathrm{L}}^2\omega_{\mathrm{c}}^2 + \omega_{\mathrm{T}}^2[\omega_{\mathrm{p}}^{(3)}(q)]^2\gamma_\pm\}]\!]^{1/2}/2 \tag{27}$$

with

$$\gamma_\pm = (S \pm S')B + (A - B). \tag{28}$$

Note that equation (27) yields four branches, since the $\pm$ sign in front of the radical is uncorrelated with the $\pm$ subscripts on γ. In the weak-coupling limit we obtain localised *3D magnetoplasmon–optical phonon modes* [11]. In the strong-coupling limit, we obtain *coupled effective 3D optical phonon magnetoplasmons* and *coupled optical phonon–acoustical magnetoplasmon modes* when $k_z = 0$. When $k_z d = (2n+1)\pi$, we find *coupled optical phonon–acoustical magnetoplasmon modes*. All these are shown in figure 3 for $\omega_{\mathrm{c}} = 0$. The pure effects of electron–phonon coupling can easily be calculated by setting $\omega_{\mathrm{c}} = 0$ in equation (27), and the cyclotron–plasmon modes can be easily acquired by letting $\omega_{\mathrm{L}} = \omega_{\mathrm{T}} = 0$ in equation (27). Finally, we consider the effects of the electron–phonon coupling and external magnetic field on the inter-sub-band modes. The pure effects of electron–phonon coupling are given by

$$\omega^2 = [\omega_{\mathrm{L}}^2 + \Omega^{(3)2}_{10} + 2\alpha^{(3)}\Omega^{(3)2}_{10}\beta_\pm/qd]/2 \pm \{[\omega_{\mathrm{L}}^2 + \Omega^{(3)2}_{10} + 2\alpha^{(3)}\Omega^{(3)2}_{10}\beta_\pm/qd]^2 - 4[\omega_{\mathrm{L}}^2\Omega^{(3)2}_{10} + 2\alpha^{(3)}\Omega^{(3)2}_{10}\omega_{\mathrm{T}}^2\beta_\pm/qd]\}^{1/2}/2 \tag{29}$$

with

$$\beta_\pm = (S \pm S')Q + (P - Q). \tag{30}$$

In the weak-coupling region ($qd \gg 1$), we have *localised 3D inter-sub-band mode and longitudinal optical plasmons*. In the strong-coupling limit ($qd \ll 1$), we have the *combined optical phonon–interface state inter-sub-band modes*, for $k_z = 0$. When $k_z d =$

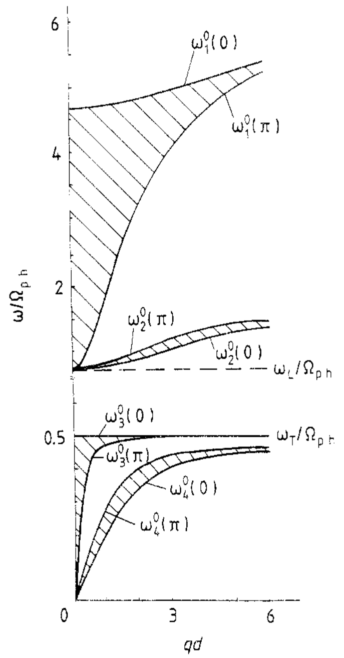

Figure 3. The collective intra-sub-band excitation spectrum for phonon–plasmon modes with the parameters $kd = 0.7742$, $\varepsilon_\infty = 16.0$, $\omega_{pe}^2/\omega_{ph}^2 = 15.0$, $(\omega_L/\Omega_h)^2 = 0.5$ and $(\omega_T/\Omega_h)^2 = 0.25$.

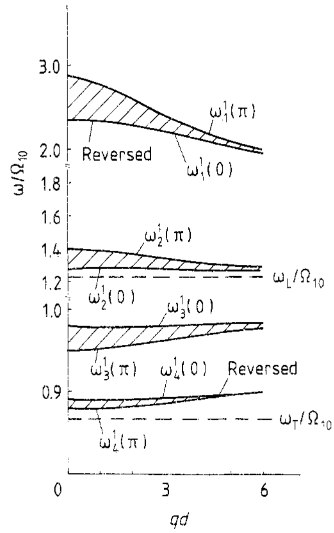

Figure 4. The collective inter-sub-band excitation spectrum for phonon–plasmon modes with the parameters $kd = 0.7742$, $\varepsilon_\infty = 16.0$, $(\alpha_e/\alpha_{lh}) = 17.5$, $(\omega_L/\Omega_{10})^2 = 1.5$, $(\omega_T/\Omega_{10})^2 = 0.75$ and $\alpha_{lh} = 1.84$.

$(2n+1)\pi$, the coupling has been screened out, as shown in figure 4. Next, we consider the effects of magnetic field; thus the first-order approximate solution can be written as

$$\omega^2 = \omega_L^2 + \{[2\alpha^{(3)}\Omega_{10}^{(3)2}\beta_\pm(1+\theta_\pm q^2)/qd](\omega^2 - \omega_T^2)\} \times \{\alpha_\pm - [2\alpha^{(3)}\Omega_{10}^{(3)2}\beta_\pm(1+\theta_\pm q^2)/\hbar]\}^{-1} \tag{31}$$

with

$$\alpha_\pm = [\omega_L^2 - \Omega_{10}^{(3)2} + 2\alpha^{(3)}\Omega_{10}^{(3)2}\beta_\pm/qd]/2 \pm \{[\omega_L^2 + \Omega_{10}^{(3)2} + 2\alpha^{(3)}\Omega_{10}^{(3)2}\beta_\pm/qd]^2 - 4[\omega_L^2\Omega_{10}^{(3)2} + 2\alpha^{(3)}\Omega_{10}^{(3)2}\omega_T^2\beta_\pm/qd]\}^{1/2}/2 \tag{32}$$

and

$$\theta_\pm = [L_H^2\alpha_\pm/4\Omega_{10}^{(3)}][(\pi L_H^2 n^{(3)} + 3)\Omega_+/(\alpha_\pm - \omega_c^2 - 2\omega_c\Omega_{10}^{(3)}) - (\pi L_H^2 n^{(3)} + 1)\Omega_-/(\alpha_\pm - \omega_c^2 + 2\omega_c\Omega_{10}^{(3)})]. \tag{33}$$

Here we have four sets of modes, since the $\pm$ subscripts on β are uncorrelated with the $\pm$ subscripts on α or θ. L_H is the Landau radius. In the long-wavelength limit, it can easily be seen that the approximate method used here will be good and sufficient.

Addendum

In this paper, we have introduced the symbols $\boldsymbol{q}$, $\boldsymbol{k}$, k_z, ω_c, ω_{pe} and ω_{ph}. Here, these symbols have the same definitions as in [10]. The symbols, κ_{HgTe}^{-1} and κ_{CdTe}^{-1} are the localisation lengths of the interface states in the materials HgTe and CdTe, respectively. The assumption that $\kappa_{HgTe} = \kappa_{CdTe}$ is made for convenience. Indeed, κ_{HgTe} is not equal to κ_{CdTe} but, if the period of the superlattice is larger than κ_{HgTe}^{-1} and κ_{CdTe}^{-1}, we think the assumption $\kappa_{HgTe} = \kappa_{CdTe}$ may not give large errors in the calculation. In the presence of a magnetic field perpendicular to the layers, quantisation along the superlattice direction (z direction) is not affected by the presence of a magnetic field. Thus the interface states referred to the quantisation in the z direction remain unchanged. In this case, the polarisability here is the same as that in [10]. The word 'Reversed' in figure 2 means that the edges of the lower branches $\omega_-(0)$ and $\omega_-(\pi)$ are interchanged compared with that in a type I superlattice. The terms A, B and C in equations (1) and (2) are additional terms coming from the overlap of the wavefunctions of the interface states at the interfaces of the superlattice.

Acknowledgments

This work was supported in part by the Chinese Higher Education Foundation through Grant 2-1987 and in part by the Chinese Science Foundation through Grant 1860723.

References

[1] Mukherji D and Nag B R 1957 *Phys. Rev.* B **12** 4338
[2] Chang Yia-Chung, Schulman J N, Bastard G, Guldner Y and Voos M 1985 *Phys. Rev.* B **31** 2557
[3] Jaros M, Zoryk A and Ninno D 1987 *Phys. Rev.* B **35** 8277
[4] Lin-Liu Y R and Sham L J 1985 *Phys. Rev.* B **32** 5561
[5] Bastard G 1982 *Phys. Rev.* B **25** 7584
[6] Faurie J-P 1986 *IEEE J. Quantum Electron.* **QE-22** 1656
[7] Berroir J M, Guldner Y and Voos M 1986 *IEEE J. Quantum Electron.* **QE-22** 1793
[8] Huang Danhong and Zhou Shixun 1988 *Phys. Rev.* B **38** 13061
[9] Sarma S D and Quinn J J 1982 *Phys. Rev.* B **25** 7603
[10] Tselis A C and Quinn J J 1984 *Phys. Rev.* B **29** 3318
[11] Burstein E, Pinczuk A and Mills D 1980 *Surf. Sci.* **98** 451